



Controlled Environment Systems Research Facility  
Guelph, Ontario CANADA  
N1G 2W1  
Tel. (519) 824-4120  
Fax. (519) 767-0755

**MELLiSSA**

**Memorandum of Understanding  
ECT/FG/MMM/97.012**

**Technical Notes 53.2 and 53.3**

Development of Nutrient and Water Dynamics Models in Higher Plant  
Chambers Based on Net Carbon Exchange Rate (NCER)

**Version 1**

**Issue: 0**

**Waters G., Dixon, M.A.**

**University of Guelph**

**January 2003**

## Table of Contents

Abstract	1
Introduction	1
Materials and Methods	4
Results	10
Discussion and Conclusion	13
Acknowledgements	14
References	14

### List of Tables

Table 1	17
Table 2	18
Table 3	19
Table 4	20
Table 5	21
Table 6	21
Table 7	22
Table 8	23
Table 9	24
Table 10	25
Table 11	26
Table 12	26
Table 13	27

### List of Figures

Figure 1	28
Figure 2	29
Figure 3	30
Figure 4	31
Figure 5	32
Figure 6	33
Figure 7	34
Figure 8	35
Figure 9	36
Figure 10	37
Figure 11	38
Figure 12	39
Figure 13	40
Figure 14	41
Figure 15	42

<b>Acronyms and Abbreviations</b>	<b>43</b>
-----------------------------------	-----------

<b>Appendix 1</b>	<b>45</b>
-------------------	-----------

# Development of Nutrient and Water Dynamics Models in Higher Plant Chambers Based on Net Carbon Exchange Rate (NCER)

Geoffrey C.R. Waters, Mike A. Dixon  
Controlled Environment Systems Research Facility,  
Department of Environmental Biology, University of Guelph,  
Guelph, Ontario, CANADA, N1G 2W1  
waters@ces.uoguelph.ca

## Abstract

This paper develops a model of nutrient and water dynamic in higher plant chambers based on Net Carbon Exchange Rate (NCER). It defines a functional relationship between the relative growth rate of beet and lettuce stands, as inferred from NCER, and relative nutrient uptake using simple linear regression. No significant differences were observed between model derived relative growth rate and relative nutrient uptake for nitrate, phosphate, ammonium, sulphate, calcium, magnesium, sodium, and potassium in beet or lettuce stands. Evapo-transpiration was also highly correlated with carbon gain. These results indicate that the technique may be a promising means to predict mass dynamics from that of carbon. Applications of the modeling approach include the development of hybrid solution management algorithms in tandem with specific ion sensors and the management of nutrient solutions under complicated (e.g. integrated, multiple physiological stages) crop production scenarios.

## Introduction

Previous work has defined the composition and cost of a baseline plant production system for life support applications as well as having established the framework for predicting and modeling mass dynamics under complicated production scenarios (Cloutier *et al.*, 1998; Waters *et al.*, 2002). This paper begins with the empirical development of scalable models of nutrient uptake and evapotranspiration in even aged monocultures. As discussed in Cloutier *et al.*, (1998), models of Net Carbon Exchange Rate (NCER), evapotranspiration and nutrient uptake can assist in the design BR systems and in formulating specific algorithms for the management of potable water fluxes, air revitalization and nutrient requirements of plant stands.

A number of attempts have been made at modeling nutrient, carbon and water dynamics in protected agriculture scenarios and life support systems (Volk and Rummel, 1987; Bloom, 1996; Pitts, 1997). Volk and Rummel (1989) modeled transpiration of wheat grown under controlled conditions as a function of inedible biomass and age. Their mechanistic model utilized separate growth models for inedible and edible biomass and relied on destructive estimation of crop yield and growth model outputs rather than instantaneous measures of plant carbon gain. Other models having application in greenhouse production include those of Jolliet and Bailey (1992), Klaring *et al.* (1997), Mankin *et al.*, (1998) and Boulard and Wang (2000). These models, too, are highly mechanistic and required input of many climatic variables.

Silberbush and Barber (1983) proposed a mechanistic model of nutrient uptake. This model made use of eleven plant and root zone variables and was far too complicated in form to be easily implemented as part of a control system for nutrient management, partially because of the number of independent variables, its independence of whole plant carbon gain and yield, and its theoretical nature.

Ideally, mass dynamics in life support systems could be expressed as a function of a single variable. An obvious candidate is the stand NCER. Estimations of NCER, or its daily integral daily carbon gain (DCG), are achieved by monitoring net CO<sub>2</sub> exchange rate in an open (flow-through) or closed chamber using in-line Infrared Gas Analysis. The net C gain (in moles) can be determined from the net removal of CO<sub>2</sub> from the chamber atmosphere (Dutton *et al.*, 1988). Net C gain is then used to calculate

stand biomass using the fact that roughly 40% of plant biomass is composed of C (Bate and Canvin, 1971; Dutton *et al.*, 1988). In addition to their non-destructive nature, and since they are highly correlated with dry weight gain, NCER estimators are a suitable measure for the effects of environment variables such as light, humidity, temperature and atmospheric CO<sub>2</sub> concentrations on crop yield (Peterson and Zelitch, 1982; Dutton *et al.*, 1988). As such, NCER responds to aggregate of a host of environmental variables and may be used to simplify models of mass dynamics in life support systems.

A practical approach to modeling nutrient uptake dynamics makes use of the concept of steady state nutrition proposed by Ingestad and Agren (1988). This assumes constant nutrient concentrations in plant tissue regardless of its physiological stage. This theory has been used by Willits *et al.*, (1992) and Mankin and Fynn, (1996) as a basis for either empirical or mechanistic models. In none of the empirical models was NCER used as a predictor variable. In these cases measures of plant yield and growth were derived from destructive harvests of plant material and these measures, in turn, were used to determine plant relative growth rate as a predictor variable.

The theory of steady state nutrition indeed provides a basis for the modeling of nutrient dynamics using knowledge of gas exchange dynamics in the aerial environment. It can be shown by that non-destructive estimations of crop RGR can be determined from NCER as follows:

$$RGR(t) = \frac{NCER(t)}{\int_{t=0}^t NCER(t) \cdot dt} \quad [1]$$

where NCER(t) is an instantaneous estimate of plant Net Carbon Exchange Rate at any age t. Equation [1] has the same form as the generic RGR equation given as:

$$RGR = \frac{dW}{dt} \cdot \frac{1}{W} \quad [2]$$

where W is the total moles of Carbon or dry biomass accumulated by a plant stand. This fact, as will be discussed in the materials and methods section, makes the ln (natural log) transform useful in deriving RGR estimates from integrated NCER values.

Ingestad and Agren's (1988) concept of steady state nutrition states that Relative Nutrient Uptake Rate (RUR) is equivalent to RGR. Relative Nutrient Uptake Rate is defined as:

$$RUR_h = \frac{U_h(t)}{\int_{t=0}^t U_h(t) \cdot dt} \quad [3]$$

where RUR<sub>η</sub> is the Relative Uptake Rate of ion or nutrient η, and where U<sub>η</sub>(t) is the instantaneous uptake rate of any ion, η, at time t. Under the assumption of steady state nutrition, the ion uptake rate, U<sub>η</sub>(t) may be estimated by non-destructive means as follows:

$$U_h(t) = \frac{NCER(t)}{\int_{t=0}^t NCER(t) \cdot dt} \cdot \int_{t=0}^t U_h(t) \cdot dt \quad [4]$$

where the variable definitions are as above.

Ingestad and Agren (1988) explain that the theory of steady state nutrition holds only if two conditions are met

- i) the relative proportions of different plant parts (tuber, roots, flowers etc.), whose mineral concentrations may differ, remains constant during the period of study,
- ii) the nutrient composition of each different plant part must itself remain constant or the relative proportions of the plant parts adjust to offset any mineral changes resulting from remobilization of any ion from one plant part to another

The implications of these conditions are that a failure to maintain a constant internal concentration of an element implies that the element was in limited supply and the plant relied on remobilization to satiate developing parts. Or, in the case of an increase in nutrient concentrations in plant tissue, there is evidence of luxuriant or over-supply of a given element. It is very difficult to confirm adherence to steady state nutrition using mineral analysis of plant parts and tissues. First, high numbers of plants must be cultured to generate sufficient biomass for analysis and secondly plant parts must be harvested at regular intervals in order to assess any drift in tissue concentrations as a result of departures in steady state theory.

The RGR and RUR should be equal under the case of steady state nutrition, and therefore a null hypothesis can be formulated as follows:

$$H_0: \frac{NCER(t)}{\int_{t=0}^t NCER(t) \cdot dt} - \frac{U_h(t)}{\int_{t=0}^t U_h(t) \cdot dt} = 0 \quad [5]$$

The testing of the null hypothesis presented in Equation [5] is the primary focus of this paper. However, a simpler form may be generally expressed as:

$$H_0: RGR - RUR = 0 \quad [6]$$

The purpose of this paper is to evaluate and demonstrate the approach to modeling mass (nutrient and water) exchange in higher plant chambers with non-destructive estimations of stand NCER as the sole predictor. In the case of modeling NCER and nutrient uptake the theory of steady state nutrition is invoked under the null hypothesis of Equation [5]. In the case of models for evapotranspiration a simple correlation with NCER is used. This paper therefore seeks to find evidence against the null hypothesis presented in Equation [5] in an effort to establish the applicability of modeling nutrient dynamic in relation to NCER.

## Materials and Methods

### Growth Chamber Facilities

For the purposes of model development at the stand level, two large sealed environment chambers capable of determining NCER of full plant stands were used. The chambers are described in detail in the paper authored by Dixon *et al.* (1997). Since the time of that original publication some changes were made to the chambers' configuration. As a result a brief description of the chambers is reproduced here. The chambers measure 4.5m x 3m and 2.5 m high. Heat exchangers and air handling equipment were integrated within the sealed environment. The glass topped chambers had externally mounted lighting with 9 x 600 W High Pressure Sodium (HPS) and 6 x 400 W Metal Halide (MH) lamps to provide a light level between 600 and 800  $\mu\text{moles m}^{-2} \text{ s}^{-1}$  PAR at stand height. For the purposes of this study, the hydroponics system described in the original paper was not used nor were the inner canopy lighting systems. The overhead lighting systems were maintained. Additionally, the original LiCor model LI6262 Gas Analyser for CO<sub>2</sub>/H<sub>2</sub>O vapour was replaced by a California Analytical Instruments O<sub>2</sub> and CO<sub>2</sub> Analyser (model 100P, Orange CA., USA). Thermal control was handled with externally supplied chilled water and steam routed through exchange coils mounted in an internal plenum at the rear of the chamber. Environment control was maintained by a computer control system (L.W. Anderson Software Consulting Ltd., Leamington, ON).

### Experimental Design

A total of five independent replications using beet and lettuce were performed at the full stand level. Three replicates were conducted using beet (*cv Beta vulgaris cv. Detroit Medium Red*) and two replicates were conducted using lettuce (*Lactuca sativa cv. Lively*). Each replicate was completed in one of the two sealed environment chambers and, if possible replications were completed simultaneously. For each replicate, 44 beet (*Beta vulgaris cv. Detroit Medium Red*) or 44 Lettuce (*Lactuca sativa cv. Lively*) were placed inside a chamber for 40 days or 21 days respectively, following a common 21 day germination period. Lettuce was selected as it is currently being investigated as a candidate crop for the ESA MELiSSA program and because rapid vegetative growth would occur during the study period, thereby simplifying the initial modeling process. Beet was selected because it, too, is currently being investigated as a candidate crop for the ESA MELiSSA program. Additionally, the beet 'root', actually an enlarged hypocotyl, was thought to provide a challenge to model development since it is a non-photosynthesizing structure.

The study described in this paper makes use of three beet and two lettuce replications with samples of nutrient uptake, evapotranspiration and NCER taken at defined intervals throughout the study period. These studies are therefore treated as an analogue of a Split-Plot Design with chamber/replication as a main factor and time as a sub-factor.

### Cultural Conditions

#### *Germination and Emergence*

For each study beet and lettuce were germinated in a research greenhouse at the University of Guelph, using Rockwool<sup>®</sup> cubes. The plants remained in the cubes for a period of 21 days or until there was sufficient root exposure to facilitate transplanting into a deep water hydroponics system. During the germination period, seedlings were watered regularly with distilled water and once weekly with a dilute fertilizer solution (20-8-20 ppm N-P-K commercial mix having an EC = 2.5 mS).

#### Hydroponics System

Following root exposure, 44 seedlings were transplanted to circular Styrofoam trays with 44 cut holes having dimensions 2.5 cm x 2.5 cm. These holes were cut from the Styrofoam trays using a razor

blade. The circular Styrofoam trays were then positioned in circular plastic pool with a surface area of 2.5 m<sup>2</sup> and having the capability to hold a volume of 220L of hydroponics solution. The Styrofoam trays were designed to float freely within the pools. Planting density was fixed at 17.6 plants m<sup>-2</sup> (44 plants per 2.5 m<sup>2</sup>). Any solution exposed to light, particularly on the margins of the Styrofoam was shielded with black plastic film to minimize the growth of algae. The pool was positioned in the center of the chamber growing area at a distance of 1.5 m from the overhead lights. The nutrient solution was continuously aerated using internal chamber air and pump. Appendix 1 is a diagrammatic representation of the hydroponics set-up.

The nutrient solution used in this study had the following composition: 1.5 mM PO<sub>4</sub><sup>3-</sup>, 3.62 mM Ca<sup>2+</sup>, 4 mM NH<sub>4</sub><sup>+</sup>-N, 11.75 mM NO<sub>3</sub><sup>-</sup>N, 5 mM K<sup>+</sup>, 2 mM SO<sub>4</sub><sup>2-</sup>, 1 mM Mg<sup>2+</sup>, 0.005 mM Mn<sup>2+</sup>, 0.025 mM Fe<sup>3+</sup> as Fe-DTPA, 0.0035 mM Zn<sup>2+</sup>, 0.02 mM B<sup>3+</sup>, 0.008 mM Na<sup>+</sup>, 0.0008 mM Cu<sup>2+</sup>, 0.0005 mM Mo<sup>6+</sup>. This solution had an average EC of 1.9 mS. The pH of the solution was adjusted to approximately 5.5 with the addition of approximately 40 mL of a 1 M NaHCO<sub>3</sub> solution per pool. At the initial transplant of the seedlings, 220 L of nutrient solution was added to the pool prior to the chamber doors being sealed. Every five days after, the chamber doors were opened to replace the older solution with a fresh 220 L volume having the same composition as noted above.

At the start of each five day solution changeover period, the total solution volume to be added was measured with a large (250 L) graduated tank and three 25 mL samples were taken of the fresh solution for off-line HPLC analysis. The old solution was pumped out of the pool and its volume measured. Samples were also taken for HPLC analysis in triplicate. Solution volumes were measured at the start and end of closure periods to allow for the correction of elemental analysis results due to evapotranspiration from the pool. During each five day closure period no amendments were made to the solution composition in any way. All solution samples were analyzed using the Dionex HPLC Model DX-120 (Sunnyvale, CA, USA) for 8 ions of interest: NO<sub>3</sub><sup>-</sup> (nitrate), PO<sub>4</sub><sup>3-</sup> (phosphate), SO<sub>4</sub><sup>2-</sup> (sulfate), K<sup>+</sup> (potassium), NH<sub>4</sub><sup>+</sup> (ammonium), Na<sup>+</sup> (sodium), Ca<sup>2+</sup> (calcium) and Mg<sup>2+</sup> (magnesium). NO<sub>2</sub><sup>-</sup> (nitrite) and Cl<sup>-</sup> (chloride) were repeatedly to be found at concentrations at or below the Dionex detection limit and so were not subjected to analysis.

#### *Environmental Conditions*

Plants were grown under static conditions of 600 μmol m<sup>-2</sup> s<sup>-1</sup> PAR lighting at stand height as supplied by the high pressure sodium and metal lamps mounted externally. A 14/10 hr light/dark (06:00 - 20:00) photoperiod was used and coupled to a 26/20 °C day/night temperature. Atmospheric CO<sub>2</sub> concentrations were fixed at 1000 μL L<sup>-1</sup> CO<sub>2</sub> as supplied through an external tank and mass flow controller. Average relative humidity in the chambers over all replications was 73% ± 5%.

#### *Harvesting*

All plant material was harvested at the end of the study for biomass determination, while NCER data was collected continuously throughout the study. Harvested material was pooled by chamber and partitioned into edible and non-edible biomass fractions. Leaf area was measured on 10 of the plants harvested using a Li-Cor 3100 Leaf Area Meter (Lincoln, NE, USA). Fresh weights were determined immediately on all plant material and dry weights were determined following 7 days in a drying oven at 65 °C. Chamber water balance was also determined from evapotranspiration estimates and plant water content estimates derived from dry and fresh plant weights.

#### Data Collection

The net carbon gain of the developing beet and lettuce stands was determined using a compensation technique. The computer controller maintained internal chamber CO<sub>2</sub> concentrations during the day-light hours so that any net carbon gain by the stand through photosynthetic activity was compensated by injections from an external tank. The volume and duration of CO<sub>2</sub> injections were used to estimate day time NCER. During the dark period it was not possible to remove CO<sub>2</sub> from the chamber to achieve static conditions and as such the difference in observed CO<sub>2</sub> and demand was used to determine

stand respiration rates (expressed as negative NCER). The sum of these NCER estimates over a 24 hour period (in moles C), yielded daily carbon gain (DCG). DCG was integrated to generate a profile of the accumulated carbon at the end of each of the five day sampling intervals. Nutrient uptake and evapotranspiration as determined from the solution sampling and changeover procedure described above were determined over the same five day interval. Uptake and evapotranspiration rates determined over the five day periods were also integrated to generate a profile of the accumulated nutrient uptake for the eight ions of interest and of accumulated evapotranspiration.

### Data Analysis

#### Data Transformation

Data analysis was conducted using the accumulated carbon profile as derived from NCER with points corresponding to the end of each of the five day sampling intervals. Analysis was also conducted in the same way for accumulated nutrient uptake. Models of nutrient uptake in relation to NCER were developed and subjected to the null hypothesis ( $H_0$ ) described in Equation [6]. Since the following equation holds:

$$RGR = \frac{dW}{dt} \cdot \frac{1}{W} \quad [7]$$

where  $W$  is biomass, integrated carbon gain or any other suitable measure of growth, RGR could be determined by taking the first derivative of a linear function fitted to the  $\ln$  transform of accumulated DCG. If  $W(t)$  is the integral of NCER from the start of the study period in the chamber to time  $t$ , then:

$$RGR(t) = \left[ \frac{d}{dt} W(t) \right] \cdot \frac{1}{W(t)} = \frac{d}{dt} \ln[W(t)] \quad [8]$$

Equation [8] shows that RGR is equal to the first derivative of the  $\ln$  transformed biomass accumulation, carbon accumulation or growth curve. Similarly, RUR is equal to the first derivative of the  $\ln$  transformed accumulated nutrient uptake function.

The accumulated carbon profile is given by the function

$$W(t) = ae^{rt} \quad [9]$$

and the accumulated nutrient uptake profile is given by:

$$A_n(t) = ce^{kt} \quad [10]$$

where  $A_n(t)$  is the accumulated nutrient uptake function. The constants  $a$  and  $c$  are unique and  $r$  and  $k$



are slopes of a linear function, representing either RGR or RUR respectively. Given Equation [9] and [4.10] it was possible to determine RGR and RUR directly through the ln transformation of Equations [9] and [10] and subsequent regression analysis to determine the first derivative parametrically. In the case of exponential growth or nutrient uptake, Equations [9] and [10] may be described generically as:

$$W(t) = \int_{t_0}^t \text{NCER}(t) \cdot dt \quad [11]$$

or

$$A_h(t) = \int_{t_0}^t U_h h(t) \cdot dt \quad [12]$$

The ln transform of Equations [11] and [12] results in a linearization to the form:

$$\ln[W(t)] = \ln(a) + rt \quad [13]$$

or

$$\ln[A_h(t)] = \ln(c) + kt \quad [14]$$

where a and c are constants and r and k are slopes of a linear function, representing either RGR or RUR respectively.

### Data Analysis Software

All data analysis described in this section was completed using the S-Plus statistical software (MathSoft, Data Analysis Products, Seattle, WA, 1999) with libraries derived from Venables and Ripley (1999).

### Regression Analysis and Model Diagnostics

Accumulated carbon and nutrient data were plotted in relation of time and assessed for an exponential pattern as given by Equations [11] and [12]. Since traces of carbon and nutrient accumulation had an exponential form (Figures 1-4) the ln transform was hypothesized to have a simple linear form as described in Equations [13] and [14]. Simple linear regression was performed on the ln transform all carbon and nutrient accumulation profiles (with the exception of lettuce  $\text{Ca}^{2+}$ ,  $\text{Na}^+$  and  $\text{SO}_4^{2-}$ , for reasons described later). The simple linear regression mode had the form:

$$\ln[W(t)] = b_1 \cdot \text{DIC} + e \quad [15]$$

or

$$\ln[A_h(t)] = b_0 + b_1 \cdot \text{DIC} + e \quad [16]$$

Equation [15] used for the accumulated carbon data was devoid of an intercept purposely for two

reasons. First, early estimates of carbon gain in the progression were inaccurate since plants were very small and the magnitudes of NCER were very small and close to the theoretical detection limit of the stand chambers, and ii) early estimates of carbon gain in the progression had to be removed due to significant leverage (see below). As such, removal of the model intercept yielded more realistic values of standing biomass at the time of closure than with the intercept included. Equation [16] was used for nutrient accumulation data. The presence of an intercept was maintained in the models since no points of high leverage could be detected and the value of the intercept was in reasonable agreement with the expected nutrient concentrations in plant tissue at door closure.

In total, 15 simple linear regressions were completed having either the form of Equation [15] or [16]. Since it is critical to the testing of  $H_0$  that the RGR and RUR estimates derived from the slope of the regressions is accurate and free from coercion, vectors of studentized residuals,  $r_i^*$ , Cook's Statistic ( $C_i$ ) and diagonal elements of the hat matrix ( $h_i$ ) were generated for each point in each regression. These quantities are indispensable in regression diagnostics and assessing the magnitude of the effects on individual points on slope estimates, known as leverage. Atkinson (1997) provides an excellent review of the utility of these statistics. Important aspects of Atkinson's (1997) discussion are repeated here.

Studentized Residuals -  $r_i^*$  - The studentized residual is a monotonic, linear function of standardized residuals. If the model holds and errors,  $\epsilon$  are normally distributed the studentized residual has a Student's t-distribution on  $n-p-1$  degrees of freedom (Atkinson, 1997). As such the statistic is a useful in detecting both the assumption of normality and in the detection of outliers. The  $r_i^*$  statistic was determined as follows:

$$r_i^* = \frac{r_i'}{s_{(i)}\sqrt{1-h_i}} = \frac{sr_i'}{s_{(i)}} \quad [17]$$

where  $s_{(i)}$  is the standard error as derived from the residual mean square estimate of  $\epsilon$  with observation  $i$  deleted and where,  $r_i'$ , the standardized residual, is given by:

$$r_i' = \frac{y_i - \hat{y}_i}{s\sqrt{1-h_i}} \quad [18]$$

where  $y_i$  is the observed response variable,  $\hat{y}_i$  is the predicted model response value,  $s$  is the standard error as derived from the residual mean square estimate of  $\epsilon$ , and  $h_i$  is the diagonal element of the hat matrix, as defined below. Because the studentized residuals have a Student's t-distribution they were plotted against an approximation of the expected value of the  $i^{\text{th}}$ -order statistic as follows:

$$E(r_{(i)}) = \Phi^{-1} \left( \frac{i - \frac{3}{8}}{n + \frac{1}{4}} \right) \quad [19]$$

where  $\Phi$  is the cumulative distribution function of the standard normal distribution,  $r_{(i)}$  is the  $i^{\text{th}}$ -order statistic of the studentized residual,  $n$  is the number of observations or residuals (Atkinson, 1997). Departures in linearity of the expected value of the order statistic indicated a departure from the normality assumption (Venables and Ripley, 1999). In cases of severe departure there is doubt that traditional

inferential procedures for parameter estimates (in this case the estimate of RGR or RUR from the ln transform) are not applicable.

Studentized residuals were also plotted as a function of the independent variable to rule out heteroscedasticity (non-constant variance).

Cook's Statistic -  $C_i$  - The studentized residuals described above were used to determine the validity of normality assumptions and for investigating the impact of a given observation on model predicted values. The studentized residuals, however, provide little information on the impact of a specific value on parameter estimates. This impact is known as leverage and is more properly investigated using the Cook's statistic,  $C_i$ . To investigate leverage,  $C_i$  was calculated as follows:

$$h_i = x_i^T (X^T X)^{-1} x_i \quad [20]$$

where  $n$  is the number of observations,  $p$  is the number of parameters estimated in the regression model,  $r_i^*$  is the studentised residual of observation  $i$  and  $h_i$  is the diagonal element of the hat matrix corresponding to point  $i$  (Atkinson, 1997). High values of the Cook's statistic indicate high leverage and instability of the regression derived RGR and RUR estimates.

Diagonal Element of the Hat Matrix -  $h_i$  - The diagonal element of the hat matrix,  $H$ , given by  $h_i$  is also a useful statistic for investigating points of leverage. If the matrix of independent variables in the regression (usually DIC) is given by  $X$  then the diagonal elements of the hat matrix is given by:

$$C_i = \left\{ \frac{n-p}{p} \cdot \frac{h_i}{1-h_i} \right\}^{\frac{1}{2}} |r_i^*| \quad [21]$$

where  $T$  is the matrix transpose. In the RGR model without intercept the  $X$  matrix is in fact a vector of DIC values. The diagonal element of the hat matrix is a measure of the remoteness of one observation,  $i$ , from the remaining  $n-1$  observations in space of the  $X$  carriers. An observation having high leverage has a value of  $h_i$  of close to unity. Values of  $h_i$  were determined for each point used in each regression and examined for magnitude. Values of  $h_i$  which were greater than  $2p/n$  were identified as having high leverage and were removed from the regression models. This occurred for only 3 points in the RGR model at locations adjacent to the start of chamber closure.

#### Non-Parametric Bootstrap Methods

In the case of the Beet data sets, a slight departure from normality was detected in the normal plots of the studentized residuals. While this departure may be consistent with the Student's  $t$  distribution of the studentized residual statistic, the absence of tailing in the lower order statistics suggested the need for non-parametric inferential approaches (Draper and Smith, 1998). Standard inferential techniques for estimating the variability of model parameter estimates (in this case RGR and RUR as derived from the slope of the ln transform model) were therefore of limited use. The non-parametric bootstrap methods as described by Efron (1987), Efron and Tibshirani (1986), Freedman (1981), Freedman and Peters (1984), and Léger *et al.* (1992). Bootstrapping of the regression model parameter estimates involved the following steps:

- i) fitting of the original full model and obtaining the full vector of residuals
- ii) taking a sample with replacement of  $n$  residuals from the full vector

- iii) adding the residual vector to the predicted model response vector
- iv) refitting the modified vector of predicted responses to generate a new estimate of the regression slope (in this case either RGR or RUR)
- v) repeating steps ii-iv 1000 times to generate a frequency distribution of the bootstrap slope (RGR or RUR) estimate
- vi) determining the 2.25% and 97.25% quantiles from the distribution of the parameter estimates to generate a 95% confidence interval.

The bootstrap derived confidence intervals, RGR\* and RUR\* were then examined for overlap. Overlap of the confidence intervals for RGR\* and RUR\* was in support of the null hypothesis presented in Equation [6] at the p=0.05 level.

### Standard Inferential Methods

In the case of lettuce data where the plots of studentized residuals suggested no violation of the normality assumption, standard inferential methods for regression analysis were used. These methods were also used for the beet data sets and compared to the bootstrap derived estimates, for academic purposes. The standard inferential approaches allowed for the determination of confidence intervals for parameter estimates (RGR and RUR) on the assumption that the error vector,  $\epsilon$  was normally distributed. The estimate  $s$  of  $\sigma$  as derived from the mean squared error estimate was used as follows:

$$b_1 \pm \frac{t\left(1-\frac{\alpha}{2}, n-2\right)s}{\left\{\sum_{i=1}^n (X_i - \bar{X})^2\right\}^{\frac{1}{2}}} \quad [22]$$

where  $t(1-\frac{\alpha}{2}, n-2)$  is the  $100(1-\frac{\alpha}{2})\%$  percentage point of the  $t$ -distribution with  $n-2$  degrees of freedom on which the estimate of  $s$  is based. The estimate  $s$  was based on the mean squared error having either  $n-2$  degrees of freedom if the intercept was in the model and  $n-1$  degrees of freedom if the intercept was removed.

## Results

A summary of basic harvest data, including mean total fresh and dry weights of beet plants taken from two replicates is provided in Table 1. Water content of tissue and leaf area are also presented. There is a strong agreement (within 10%) of integrated carbon uptake estimates of biomass gain and those observed at harvest (Table 1).

The profile of the  $\ln$  transformed accumulated carbon for the full beet stand of 44 plants is presented in Figure 1. The profiles of nutrient accumulation in the full beet stand of 44 plants is presented in Figures 1-4. These figures correspond to the accumulation profile of  $\text{NO}_3^-$  and  $\text{PO}_4^{3-}$  (Figure 1),  $\text{Mg}^{2+}$  and  $\text{K}^+$  (Figure 2),  $\text{Ca}^{2+}$  and  $\text{SO}_4^{2-}$ , (Figure 3) and  $\text{NH}_4^+$  and  $\text{Na}^+$  (Figure 4). The  $\ln$  transform data for  $\text{C}^{4+}$  is reproduced on each of these plots to facilitate visual comparison of slopes.

It is important to note the underlying assumption which validates the use of a single and constant RGR or RUR throughout the crop growth period. The data collected in both the lettuce and beet trials are for the periods during which vegetative growth was occurring. In fact, data were not collected for the reproductive phases of these crops since they are leafy green vegetables whose edible portion is purely vegetative. Growth of vegetative plant parts is typically exponential in profile (Causton and Venus, 1981).

Given the exponential characteristics of both the nutrient accumulation and growth profiles for both the beet and lettuce crop, it is justifiable to assume a constant RGR and RUR throughout the vegetative period. The assumption of a constant RGR or RUR is not necessarily appropriate in cases where crops are grown until anthesis or the onset of flowering.

A further challenge in correlating RGR and RUR is in the fact that RGR is derived from integrated DCG. Because DCG is variable due to a number of factors (including slight errors in infra-red gas analysis, a lag plant response to illumination) it is difficult to achieve correlations directly between RGR and RUR through NCER estimations. Further, similar arguments can be made with respect to the estimation of nutrient uptake, especially during the early phases of growth when uptake is small. Thus, variability inherent in the DCG and uptake profiles was first partially reduced with the primary regression of the ln transform of the accumulated biomass and nutrient uptake profiles on DIC. This allowed for a reduction in variability and the direct comparisons of RGR and RUR through an examination of confidence intervals (since a t-test is not strictly valid in this case given that  $s$  for both samples is unknown and can not be assumed equal). It is for these reasons that the use of constant RGR and RUR estimates derived from regression on the ln transformed data is appropriate here.

Tables 2 and 3 summarize the results of the regression analyses performed on the ln transformed accumulated uptake of these masses. In the case of the simple linear regressions performed on the ln transforms of accumulation profiles, all models were significant. The calculated p-values for slope estimates ( $b_1$ ) were smaller than 0.05 and in most cases high coefficients of determination ( $r^2$ ) were observed. All models had small residual standard errors, and in the case of nutrient profiles, the intercept term was significant.

In the case of ln transformed models for beet nutrient and carbon accumulation, some departure from normality of the residuals was noted based on normal quantile plots. Since inferences made on slope estimates using classical regression techniques demand the assumption of normality, the non-parametric bootstrap approach to deriving confidence intervals for slope estimates was employed. Examples of the bootstrap results are presented in Figures 5-9. These density plots present both the observed and smoothed density estimators for bootstrap values of the predicted regression slopes. Because these slopes were of ln transformed data, they also represent estimators of RGR (in the case of carbon) or RUR (in the case of other nutrients). On each bootstrap density plot are the 2.5% and 97.5% quantiles for the estimates, thereby defining a 95% confidence interval. In addition, bootstrap density plots for the RUR estimators include the quantiles for the RGR estimate as presented in Figure 5. This allows for easy detection of overlap between confidence intervals derived for RUR and RGR. While the bootstrap density plots are presented only for carbon, nitrate, ammonium, potassium and phosphate, the derived quantiles are presented for all nutrients in Table 2. In addition, the confidence intervals derived through classical inferential techniques as presented in Equation [22] are presented. Excellent correspondence between the slope estimates of the non-parametric or distribution free, bootstrap approach and the standard inferential approach are observed. This finding indicates that the normality assumption of regression was indeed not violated in any of the ln transform models.

Of particular importance is the fact that in all cases the regression derived confidence intervals or the bootstrap derived quantiles of RUR overlap the same estimates for RGR. As such there is no evidence against the null hypothesis against the null hypothesis presented in Equation [6]. As such for the case of beet, no significant differences between NCER derived estimates of RGR and RUR are apparent.

Table 4 summarizes the model predicted and mean observed accumulations in nutrients and carbon as well as the accumulation expressed as a percentage of total supply over the study period. In most cases less than 50% of the supplied nutrient was consumed, with 79% of the ammonium supplied consumed. Given the modest to low rates of consumption percentage, it is likely that no element was deficient over the course of the study. This is supported by adherence to steady state nutrition theory. In addition to the percent consumption values, the accumulation ratio of nutrient uptake, expressed as total moles uptake per mole of carbon accumulated is presented for each ion. For most macro-nutrients, this ratio was near 0.10, although for phosphate it was a much lower 0.01. Micronutrients had an

accumulation ratio of 0.01 in all cases.

Over the course of crop development, it was estimated that nearly 12863 moles of water were utilized as a result of evapo-transpiration and plant accumulation (Table 4). It was determined that the crop held 687 moles of water at harvest (from dry and fresh weight measurements). Therefore a total of 12176 moles of water loss from the reservoir is due to evapo-transpiration in the beet stand directly.

Results of the simple linear regression of water use on DCG are presented in Table 5. Significant models were obtained for total water use and transpiration and water accumulation in tissue as a function of accumulated carbon. Significant relationships between total water usage and Days in Chamber were also observed for the beet stand. Estimates of the slope derived from the regression of the ln transform of accumulated water use and carbon gain are presented in Table 6. This value is referred to as the Water Use Efficiency of productivity. Figure 10 presents the profile of ln transform of accumulated water use as a function of DIC for the beet stand. As is evidenced by the values in Table 5, this model is significant.

A summary of harvest data, including mean total fresh and dry weights of lettuce plants taken from two replicates is provided in Table 7. Water content of tissue and leaf area are also presented. There is a strong agreement (within 10%) of integrated carbon uptake estimates of biomass gain and those observed at harvest.

The profiles of nutrient accumulation in the full lettuce stand of 44 plants is presented in Figures 12 –14. These figures correspond to the accumulation profile of  $\text{NO}_3^-$  and  $\text{PO}_4^{3-}$  (Figure 11),  $\text{Ca}^{2+}$  and  $\text{SO}_4^{2-}$ , (Figure 12),  $\text{Mg}^{2+}$  and  $\text{K}^+$  (Figure 13), and  $\text{NH}_4^+$  (Figure 14). Plots for the ln transform of  $\text{Na}^+$  accumulation are not presented, because poor uptake profiles were observed.

Tables 8 and 9 summarize the results of the regression analyses performed on the ln transformed accumulated uptake of these masses. In the case of the simple linear regressions performed on the ln transforms of accumulation profiles, only models for nitrate, ammonium, phosphate, potassium and magnesium were significant. The calculated p-values for slope estimates ( $b_1$ ) in those cases were smaller than 0.05. Despite the models' significance, comparatively low coefficients of determination ( $r^2$ ) were observed (ranging from 0.49 to 0.86 in significant models). No significant departures in the normality assumption of residuals were observed and so the non-parametric bootstrap procedure was not employed.

In most, but not all cases, the regression derived confidence intervals of RUR overlap the same estimates for RGR. Exceptions are estimates for ammonium and sodium. As such, there is no evidence against the null hypothesis presented in Equation [6] for RUR of nitrate, phosphate, potassium, magnesium, calcium or sulphate. For the additional case of lettuce, no significant differences between NCER derived estimates of RGR and RUR are apparent for those ions.

Table 10 summarizes the model predicted and mean observed accumulations in nutrients and carbon as well as the accumulation expressed as a percentage of total supply over the study period. In all cases less than 20% of the supplied nutrient was consumed by the lettuce crop. Given the low rates of consumption percentage, it is likely that no element was deficient over the course of the study but that such low uptake rates made model development, especially for the cases of ammonium and sodium, very difficult.

In addition to the percent consumption values, the accumulation ratio of nutrient uptake, expressed as total moles uptake per mole of carbon accumulated is presented for each ion. For nitrate and potassium, this ratio was near 0.10. The ration was considerably lower for phosphate, ammonium and the micro-nutrients.

Over the course of crop development, it was estimated that nearly 5526 moles of water were utilized by the lettuce stands, on average (Table 10). It was determined that the crop held 233.8 moles of water at harvest (from dry and fresh weight measurements). Therefore a total of 5292 moles of water loss

from the reservoir is due to evapo-transpiration in the lettuce stand directly.

Results of the simple linear regression of water use on DCG are presented in Table 11 for the lettuce stand. Significant models were obtained for total water use and transpiration and water accumulation in tissue as a function of accumulated carbon. A significant relationship between total water usage and Days in Chamber (DIC) were also observed for the lettuce stand. Estimates of the slope derived from the regression of the ln transform of accumulated water use and carbon gain are presented in Table 12. This value is referred to as the Water Use Efficiency of productivity. Figure 15 presents the profile of ln transform of accumulated water use as a function of DIC for the lettuce stand. As is evidenced by the values in Table 5, this model is significant.

Results from the post-harvest analysis of tissue samples and nutrient contents collected at harvest for both beet and lettuce trials is presented in Table 13. This table includes mineral concentrations for carbon, nitrogen, calcium, phosphorus, potassium, magnesium, sulphur and ash. These values represent means of three replicates taken from plant material pooled over all chambers at harvest.

## Discussion and Conclusion

In general there is good agreement between RGR estimates derived from NCER estimates of crop growth and RUR as determined from accumulated nutrient uptake profiles from hydroponics reservoirs. The relationship between RGR and RUR was strong in beet data but substantially weaker in the lettuce data. The agreement of RUR and RGR is consistent with the hypothesis of Ingestad and Agren (1988) and the findings of Willits *et al.* (1992). The findings of Willits *et al.* (1992) were based on RGR determinations derived from classical growth analysis. Willits *et al.* (1992) found that for nitrogen, phosphorus, potassium and manganese, the RUR for each element had a mean near 0.10. While those findings were derived from studies on Chrysanthemum, they have the same magnitude as results obtained in this study for beet and lettuce. Additionally, Willits *et al.* (1992) examined the relationship between RUR and time. This was done since Chrysanthemum, as a flowering crop, had non-constant RGR throughout its growth cycle.

An additional cautionary note is appropriate when the theory of steady state nutrition is applied to short rotation crops such as beet and lettuce (Ingestad and Agren, 1988), since the theory was originally developed for longer rotation forest crops. Initially, assimilate sinks in beet and lettuce are small and growth of these plant parts (enlarged hypocotyls, roots) is delayed until assimilate source strength (in the canopy) increases to supply escalating carbon demands of the non-photosynthetic sink parts (enlarged hypocotyls, roots). Therefore, using a proportional model for assimilate partitioning, such as that of Grodzinski *et al.* (1996), and Reekie *et al.* (1998) there is the implication of a delay in growth of major sinks. Further, as the beet or lettuce canopy matures and assimilate source supplies begin to diminish (due to later stage decreases in RGR), there may be an additional lag before depressions in the RGR of sink parts are observed. This further implies that during very early or late phases of stand development, the adherence to steady state nutrition may not be observed. In longer rotation crops, these effects are likely diminished. When using empirical data for modeling relationships between RGR and RUR, the analyst should be aware of data points having influence on regression parameter estimates during the early and late phases of stand development. This was done in this study and the results are therefore consistent with the theory of steady state nutrition.

The poorer performance of models predicting RUR and nutrient accumulation in lettuce crops may be due to the relatively low consumption percentages, as presented in Table 10. At low magnitudes of uptake it is difficult, over a 5 day interval, to accurately measure ion depletion in samples taken from solution reservoirs. While it may have been possible to extend the solution sampling period beyond 5

days in hopes of achieving a higher magnitude of uptake this would reduce the number of points represented in the uptake profile rendering resulting models less reliable. The excellent agreement between observed carbon gain and biomass at harvest for both crops, suggests that the RGR estimate is sound.

Significant models of water accumulation could be determined for both crops. Of particular interest is the Water Use Efficiency of Productivity estimates collected for both crops. These values are consistent with the mean WUEPr for *G* plants of between 1.4 and 2.5 g Carbon kg H<sub>2</sub>O<sup>-1</sup> (Larcher, 1995). It is important to note that these values were obtained for a batch planted stand. This fact becomes important when comparisons are made with staged stands later in this work.

There is the possibility of developing a control system which includes NCER as a predictor of instantaneous nutrient uptake rates. It is envisioned that empirical models could be included in a control system, along with sufficiently advanced ion specific sensors to provide elements of predictive control and aberrance detection (Cloutier *et al.* 1997).

While the work presented in this paper focused on a crop grown under static environmental conditions, in theory, it is also possible to develop models of uptake in relation to variable environment conditions. This may be done via NCER dynamic which is itself highly correlated with these variables. This approach may also prove to be particularly useful in cases of integrated crop production.

In complicated production scenarios which may include multiple crops in a common atmosphere and nutrient solution, it is the behaviour of the whole stand that is of importance. If we assume that the theory of steady state nutrition holds for all crops within the production scenario (this would be confirmed on a monoculture basis) then it is possible to develop models for nutrient uptake based on the aggregate NCER and the gas dynamics of the complicated stand.

In summary, the relationship between NCER and relative growth rate may prove to be a means of modeling nutrient and water dynamics in closed systems using a single variable, that of carbon gain.

## Acknowledgements

The senior author is very much grateful for the generous funding he has received. These include, the Natural Sciences and Engineering Research Council Industrial Post Graduate Fellowship (NSERC-IPGS), additional NSERC-IPGS support from AlliedSignal Aerospace (Honeywell), the University of Guelph Soden Memorial Fellowship in Agriculture, the University of Guelph Mary Edmunds Williams Fellowship, the Agriculture and Agri-food Canada Research Fellowship, the Centre for Research in Earth and Space Technology (CRESTech) Industrial Co-operative Research Fellowship, and the CRESTech Travel Award. The additional grant support of CRESTech, the European Space Agency MELiSSA program, Environment Canada, Flowers Canada, Ontario, and the Ontario Ministry of Agriculture, Food and Rural Affairs is also greatly appreciated.

## References

- Atkinson, A. C. (1997), Plots, transformations and regression: an introduction to graphical methods of diagnostic regression analysis. Clarendon Press, Oxford, pp. 1-79.
- Bate G.C. and Canvin D.T. (1971), "A gas exchange system for measuring the productivity of plant populations in controlled environments," *Canadian Journal of Botany*, 49, 601-608.



Bloom A.J. (1996), "Nitrogen dynamics in plant growth systems," *Life Support and Biosphere Science*, 3, 35-41.

Boulard T. and Wang S. (2000), "Greenhouse crop transpiration model from external climate conditions," *Acta Horticulturae*, 534, 235-244.

Causton D.R. and Venus, J.C. (1981), "The Biometry of Plant Growth," Edward Arnold Publishers, London.

Cloutier G.R., Cote R., Stasiak M., Dixon M.A., and Arnold K.E. (1998), "Physiological aspects of integrated crop production in advanced life support systems," *Society of Automotive Engineers Technical Paper Series*, 981561.

Cloutier G.R., Dixon M.A., and Arnold K.E. (1997), "Evaluation of sensor technologies for automated control of nutrient solutions in life support systems using higher plants," *6th European Symposium on Space Environmental Control Systems*, Noordwijk, The Netherlands.

Dixon M.A., Grodzinski B., Cote R., and Stasiak M. (1997), "Sealed environment chamber for canopy light interception and trace hydrocarbon analyses," *Advances in Space Research*, 24, 271-280.

Draper N.R. and Smith S., (1998), *Applied regression analysis*. John Wiley and Sons Inc., New York, pp. 179-216.

Dutton R.G., Jiao J.K., Tsujita M.J., and Grodzinski B. (1988), "Whole plant CO<sub>2</sub> exchange measurements for non-destructive estimation of growth," *Plant Physiology*, 86, 355-358.

Efron B. (1987), "Better bootstrap confidence intervals," *Journal of the American Statistical Association*, 85, 79-89.

Efron B. and Tibshirani R.J. (1986), "Bootstrap methods for standard errors, confidence intervals and other measures of statistical accuracy," *Statistical Science*, 1, 54-77.

Freedman D.A. (1981), "Bootstrapping regression models," *The Annals of Statistics*, 9, 1218-1228.

Freedman D.A. and Peters S.C. (1984), "Bootstrapping a regression equation: some empirical results," *Journal of the American Statistical Association*, 79, 97-106.

Grodzinski B.L., Woododrow L., Leonardos E.D., Dixon M.A., and Tsujita M.J. (1996), "Plant responses to short and long term exposures to high carbon dioxide levels in closed environments," *Advances in Space Research*, 21, 81-90.

Ingestad T. and Agren G.I. (1988), "Nutrient uptake and allocation at steady state nutrition," *Physiologica Plantae*, 72, 450-459.

Jolliet O. and Bailey B.J. (1992), "The effect of climate on tomato transpiration in greenhouses: measurements and models comparison," *Agricultural and Forest Meteorology*, 58, 43-62.

Klaring H.P., Schwarz D., and Heissner A. (1997), "Control of nutrient solution concentration in tomato crops using models of photosynthesis and transpiration: a simulation study," *Acta Horticulturae*, 450, 329-334.

Larcher, W. (1995), *Physiological Plant Ecology*, Springer, New York.

Leger C., Politis D.N., and Romano J.P. (1992), "Bootstrap technology and applications," *Technometrics*, 34, 378-398.

- Mankin K.R. and Fynn R.P. (1996), "Modeling individual nutrient uptake by plants: Relating demand to micro-climate," *Agricultural Systems*, 50, 101-114.
- Mankin K.R., Fynn R.P., and Short T.H. (1998), "Water uptake and transpiration characterization of New Guinea Impatiens," *Transactions of the American Society of Agricultural Engineers*, 41, 219-226.
- Peterson R. and Zelitch I. (1982), "Relationship between net CO<sub>2</sub> assimilation and dry weight accumulation in field grown tobacco," *Plant Physiology*, 74, 413-416.
- Pitts M. (1997), Modeling nutrient mineral transport in advanced life support systems. NASA internal report, Johnson Space Centre.
- Reekie E.G., MacDougall G., Wong I., and Hicklenton P.R. (1998), "Effect of sink size on growth response to elevated atmospheric CO<sub>2</sub> within the genus brassica," *Canadian Journal of Botany*, 76, 820-835.
- Silberbush M. and Barber, S. A. (1983), "Sensitivity of simulated phosphorus uptake to parameters used by a mechanistic-mathematical model," *Plant and Soil*, 74, 93-100.
- Venables W.N. and Ripley B.D. (1999), *Modern applied statistics with S-Plus*, Springer, New York.
- Volk T. and Rummel J.D. (1987), "Mass balances for a biological life support system simulation model," *Advances in Space Research* 7, 141-148.
- Volk, T. and Rummel, J. D. (1989), "Transpiration during life cycle in controlled wheat growth," *Advances in Space Research* 9, 61-64.
- Waters G.R., Olabi A., Hunter J.B., Dixon M.A., and Lasseur C. (2002), "Bioregenerative food system cost based on optimized menus for advanced life support," *Life Support and Biosphere Science*, 8, 199-210.
- Willits D.H., Nelson P.V., Peet M.M., Depa M.A., and Kuehny J.S. (1992), "Modeling nutrient uptake in Chrsanthemum as a function of growth rate," *Journal of the American Society of Horticultural Science*, 117, 769-774.

Table 1. Harvest data for full stand beet experiments. Data presented are means for 20 plants collected over two chambers following harvest at 33 Days In Chamber (DIC) or 54 Days After Planting (DAP) (n=20 plants). Square brackets refer to the 95% upper (UCL) and lower (LCL) 95% confidence limits of the mean respectively. Harvest data for the third replication (at 38 days DIC) are not presented. The mean leaf area per plant from harvested material collected in both chambers is presented as a bracketed value. The mean total carbon gain as calculated from integrated carbon gain is also presented along with the observed error relative to harvest estimates.

Parameter	Fresh Weight at Harvest (g plant <sup>-1</sup> )	Dry Weight at Harvest (g plant <sup>-1</sup> )	Water Content (g plant <sup>-1</sup> )
Leaves (Area, cm <sup>2</sup> plant <sup>-1</sup> )	239.6 [214.9, 264.3] (1760.4)	14.7 [13.3, 16.1]	224.9 [201.4, 248.3]
Beet Root	150.7 [123.7, 177.6]	13.6 [11.4, 15.7]	137.1 [112.2, 162.0]
Total Edible	390.3 [338.6, 441.9]	28.3 [24.7, 31.8]	362.0 [313.6, 410.3]
Total Inedible (Roots)	26.4 [22.1, 30.6]	1.7 [1.5, 1.9]	24.7 [20.6, 28.8]
Total	416.7 [360.7, 472.5]	30.0 [26.2, 33.7]	386.7 [334.2, 439.1]
Total (mol stand <sup>-1</sup> )	S	36.0 (Carbon)	Observed 34.6 (Error = -4.9%)

Table 2. Relative growth rate (RGR) and relative uptake rate (RUR) estimates and inference statistics for full stand beet experiments. The terms  $b_0$  and  $b_1$  refer to the ln-transformed model intercept and slope respectively. SLSR refers to those estimates obtained from Simple Least Squares Regression (SLSR). LCL and UCL refer to the Lower and Upper 95% confidence limits, respectively, as obtained from standard inferential techniques. RUR can be interpreted as RGR for the case of carbon.

Ion	SLSR $b_0$	SLSR RUR ( $b_1$ )	Bootstrap RUR ( $b_1$ )	2.5% Bootstrap Quantile	97.5% Bootstrap Quantile	LCL	UCL
$\text{NO}_3^-$	-2.309	0.111	0.111	0.089	0.131	0.094	0.129
$\text{NH}_4^+$	-2.930	0.093	0.093	0.074	0.116	0.075	0.110
$\text{PO}_4^{3-}$	-4.550	0.103	0.103	0.086	0.118	0.089	0.118
$\text{K}^+$	-3.361	0.135	0.135	0.110	0.171	0.112	0.159
$\text{Mg}^{2+}$	-5.206	0.121	0.126	0.102	0.171	0.010	0.154
$\text{Ca}^{2+}$	-3.791	0.084	0.084	0.052	0.119	0.045	0.123
$\text{Na}^+$	-4.619	0.101	0.102	0.080	0.132	0.076	0.126
$\text{SO}_4^{2-}$	-4.107	0.078	0.077	0.061	0.101	0.059	0.096
<b><math>\text{C}^{4+}</math></b>	n	<b>0.106</b>	<b>0.106</b>	<b>0.097</b>	<b>0.113</b>	<b>0.096</b>	<b>0.117</b>

Table 3. Model performance measures for full stand beet experiments. The  $t$ ,  $p$ , and standard error values presented are for the regression slope coefficient ( $b_1$ ). The slope estimates for these model forms corresponds to the relative uptake rate (RUR) for each ion or the relative growth rate (RGR) in the case of carbon. The  $r^2$  value includes true error.

Model Dependent Variable	t-value for $b_1$	p-value for $b_1$	Standard Error of $b_1$	$r^2$	Residual Standard Error
$\ln(A_{\text{Nitrate}})$	13.47	0.00	0.008	0.90	0.39
$\ln(A_{\text{Ammonium}})$	11.18	0.00	0.008	0.86	0.40
$\ln(A_{\text{Phosphate}})$	14.47	0.00	0.007	0.91	0.34
$\ln(A_{\text{Potassium}})$	11.9	0.00	0.011	0.88	0.51
$\ln(A_{\text{Magnesium}})$	9.77	0.00	0.013	0.83	0.59
$\ln(A_{\text{Calcium}})$	4.4	0.00	0.019	0.52	0.83
$\ln(A_{\text{Sodium}})$	8.48	0.00	0.012	0.78	0.57
$\ln(A_{\text{Sulphate}})$	8.71	0.00	0.009	0.79	0.43
<b><math>\ln(A_{\text{Carbon}})</math></b>	<b>21.2</b>	<b>0.00</b>	<b>0.005</b>	<b>0.97</b>	<b>0.51</b>

Table 4. Modeled nutrient and water accumulation data for full stand beet experiments. Bracketed values refer to the lower and upper 95% confidence intervals. Accumulation ratio refers to the moles of nutrient accumulated per mole of carbon sequestered, as calculated from model results. Water data presented is for total accumulation from pools (Total), water content in tissue as determined from harvest data (Tissue) and water lost from pools due to evapo-transpiration (ET). Total supply is calculated over the duration of the experiment. DIC refers to the number of Days in the Chamber. The observed total C<sup>4+</sup> accumulation is from integrated carbon gain estimates as presented in Table 4.1.

Ion	Model Predicted Accumulation after 34 DIC (mol)	95% CI (mol)	% of Total Supply	Accumulation Ratio after 34 DIC
NO <sub>3</sub> <sup>-</sup>	4.4	(3.4,5.6)	20	0.12
NH <sub>4</sub> <sup>+</sup>	3.5	(1.0,1.6)	79	0.10
PO <sub>4</sub> <sup>3-</sup>	0.4	(0.3,0.4)	17	0.01
K <sup>+</sup>	3.4	(2.5,4.8)	42	0.10
Mg <sup>2+</sup>	0.4	(0.3,0.6)	26	0.01
Ca <sup>2+</sup>	0.4	(0.2,0.7)	7	0.01
Na <sup>+</sup>	0.3	(0.2,0.4)	38	0.01
SO <sub>4</sub> <sup>2-</sup>	0.2	(0.2,0.3)	8	0.01
H <sub>2</sub> O (Total)	12863	(11048,14913)	15.0	n
H <sub>2</sub> O (Tissue)	687	S	0.8	n
H <sub>2</sub> O (ET)	12176	S	14.2	n
<b>C<sup>4+</sup></b>	<b>36.8</b>	<b>(27.4,49.4)</b>	S	<b>1</b>
<b>C<sup>4+</sup> (observed)</b>	<b>34.8</b>	-	-	-

Table 5. Regression results for various models of water dynamic in full stand beet experiments.  $A_{\text{water}}$  refers to the accumulated total water lost from pools,  $A_{\text{transpiration+Tissue}}$  refers to water accumulated by the canopy and lost due to transpiration. The parameters  $b_0$  and  $b_1$  refer to the model intercept and slope respectively. The  $r^2$  value includes pure error. Indep. refers to the model independent variable.

Model Dependent Variable	Indep. Variable	$b_0$	$b_1$	p- value for $b_1$	t- value for $b_1$	$r^2$	Residual Standard Error
$A_{\text{water}}$	$A_{\text{carbon}}$	788.8	325.9	0.00	77.9	0.99	250
$A_{\text{transpiration+Tissue}}$	$A_{\text{carbon}}$	0.0	325.9	0.00	77.9	0.99	250
$\ln(A_{\text{water}})$	DIC	6.30	0.09	0.00	18.8	0.95	0.23

Table 6. Water use efficiency of productivity ( $WUE_{Pr}$ ) for full stand beet experiments. Values of  $WUE_{Pr}$  were derived from the slope of regressions of  $A_{\text{water}}$  and  $A_{\text{carbon}}$ .

Variable	$\text{mol H}_2\text{O mol}^{-1} \text{C}^{4+}$	$\text{mol C}^{4+} \text{mol}^{-1} \text{H}_2\text{O}$	$\text{g C}^{4+} \text{Kg}^{-1} \text{H}_2\text{O}$
$WUE_{Pr}$	325.9	0.003	2.06

Table 7. Harvest data for full stand lettuce experiments. Data presented are means, 95% upper (UCL) and lower (LCL) confidence intervals (in square brackets) on 20 plants collected over two chambers following harvest at 24 Days In Chamber (DIC) or 45 Days After Planting (DAP). The mean total moles of carbon accumulated by the canopies is also presented. Mean leaf area of material harvested from both chambers is presented as a bracketed value. The mean total carbon gain as calculated from integrated carbon gain is also presented along with the observed error relative to harvest estimates.

Parameter	Fresh Weight at Harvest (g plant <sup>-1</sup> )	Dry Weight at Harvest (g plant <sup>-1</sup> )	Water Content (g plant <sup>-1</sup> )
Edible (Leaves) (Leaf Area cm <sup>2</sup> plant <sup>-1</sup> )	89.2 [77.1, 101.4] (1043.9)	4.3 [3.8, 4.8]	84.9 [73.2, 96.6]
Inedible (Roots)	17.4 [15.6, 19.1]	1.4 [1.2, 1.5]	16.0 [14.4, 17.6]
Total	106.6 [92.7, 120.5]	5.7 [5.0, 6.3]	100.9 [87.6, 114.2]
Total (mol stand <sup>-1</sup> )	S	7.7 (Carbon)	233.8
Total Observed Carbon Gain (mol)	–	8.0 (Carbon) (Error = +3.9 %)	–



Table 8. Relative growth rate (RGR) and relative uptake (RUR) estimates and inference statistics for full stand lettuce experiments. The terms  $b_0$  and  $b_1$  refer to the ln-transformed model intercept and slope respectively. SLSR refers to those estimates obtained from Simple Least Squares Regression (SLSR). LCL and UCL refer to the Lower and Upper 95% confidence limits as obtained from standard inferential techniques. RUR can be interpreted as RGR for the case of carbon.

Ion	SLSR $b_0$	SLSR RUR ( $b_1$ )	UCL ( $b_1$ )	LCL ( $b_1$ )
$\text{NO}_3^-$	-1.85	0.070	0.134	0.006
$\text{NH}_4^+$	-3.36	0.113	0.162	-0.207
$\text{PO}_4^{3-}$	-4.47	0.091	0.124	0.058
$\text{K}^+$	-1.63	0.070	0.113	0.029
$\text{Mg}^{2+}$	-5.31	0.082	0.139	0.026
$\text{Ca}^{2+}$	-2.43	0.043	0.116	-0.030
$\text{Na}^+$	-2.47	-0.093	0.020	-0.207
$\text{SO}_4^{2-}$	-3.62	0.053	0.121	-0.016
<b><math>\text{C}^{4+}</math></b>	n	<b>0.073</b>	<b>0.104</b>	<b>0.043</b>

Table 9. Model performance measures for full stand lettuce experiments. The t-, p-, and standard error values presented are for the regression slope coefficient ( $b_1$ ). The slope estimates for these model forms corresponds to the relative uptake rate (RUR) for each ion or the relative growth rate (RGR) in the case of carbon. The  $r^2$  value includes true error.

Model Dependent Variable	t-value for $b_1$	p-value for $b_1$	Standard Error of $b_1$	$r^2$	Residual Standard Error
$\ln(A_{\text{Nitrate}})$	2.59	0.04	0.027	0.49	0.50
$\ln(A_{\text{Ammonium}})$	5.35	0.00	0.021	0.80	0.38
$\ln(A_{\text{Phosphate}})$	6.55	0.00	0.014	0.86	0.26
$\ln(A_{\text{Potassium}})$	3.96	0.01	0.018	0.69	0.32
$\ln(A_{\text{Magnesium}})$	3.44	0.01	0.024	0.63	0.44
$\ln(A_{\text{Calcium}})$	1.41	0.20	0.031	0.22	0.56
$\ln(A_{\text{Sodium}})$	-1.91	0.10	0.048	0.34	0.89
$\ln(A_{\text{Sulphate}})$	1.84	0.11	0.029	0.33	0.52
<b><math>\ln(A_{\text{Carbon}})</math></b>	<b>6.54</b>	<b>0.00</b>	<b>0.011</b>	<b>0.91</b>	<b>0.52</b>

Table 10. Modeled nutrient and water accumulation data for full stand lettuce experiments. Bracketed values refer to the lower and upper 95% confidence intervals. Accumulation ratio refers to the moles of nutrient accumulated per mole of carbon sequestered, as calculated from model results. Water data presented is for total accumulation from pools (Total), water content in tissue as determined from harvest data (Tissue) and water lost from pools due to evapo-transpiration (ET). Total supply is calculated over the duration of the experiment. DIC refers to the number of Days in the Chamber. The observed total C<sup>4+</sup> accumulation is from integrated carbon gain estimates as presented in Table 4.7.

Ion	Model Predicted Accumulation after 24 DIC (mol)	95% CI (mol)	% of Total Supply	Accumulation Ratio after 24 DIC
NO <sub>3</sub> <sup>-</sup>	0.84	(0.50, 1.4)	0.05	0.10
NH <sub>4</sub> <sup>+</sup>	0.52	(0.35, 0.77)	0.17	0.06
PO <sub>4</sub> <sup>3-</sup>	0.10	(0.08, 0.13)	0.07	0.01
K <sup>+</sup>	1.1	(0.76, 1.5)	0.19	0.13
Mg <sup>2+</sup>	0.04	(0.02, 0.06)	0.04	0.004
Ca <sup>2+</sup>	0.25	(0.14, 0.44)	0.07	0.03
Na <sup>+</sup>	0.01	(0.003, 0.02)	0.02	0.001
SO <sub>4</sub> <sup>2-</sup>	0.09	(0.05, 0.16)	0.04	0.01
H <sub>2</sub> O (Total)	5526	(4964, 6186)	0.09	n
H <sub>2</sub> O (Tissue)	234	S	0.004	n
H <sub>2</sub> O (ET)	5292	S	0.09	n
<b>C<sup>4+</sup></b>	<b>8.4</b>	<b>(4.1, 15.6)</b>	S	<b>1</b>
<b>C<sup>4+</sup> Observed</b>	<b>8.0</b>	-	-	-

Table 11. Regression results for various models of water dynamic in full stand lettuce experiments.  $A_{\text{water}}$  refers to the accumulated total water lost from pools,  $A_{\text{Transpiration+Tissue}}$  refers to water accumulated by the canopy and lost due to transpiration. The parameters  $b_0$  and  $b_1$  refer to the model intercept and slope respectively. The  $r^2$  value includes pure error. Indep. refers to the model independent variable.

Model Dependent Variable	Indep. Variable	$b_0$	$b_1$	p- value for $b_1$	t-value for $b_1$	$r^2$	Residual Standard Error
$A_{\text{water}}$	$A_{\text{carbon}}$	2021.2	423.1	0.00	12.9	0.98	208
$A_{\text{Transpiration+Tissue}}$	$A_{\text{carbon}}$	0.0	423.1	0.00	12.9	0.98	208
$\ln(A_{\text{water}})$	DIC	6.3	0.1	0.00	17.9	0.98	0.11

Table 12. Water use efficiency of productivity ( $WUE_{Pr}$ ) for full stand lettuce experiments. Values of  $WUE_{Pr}$  were derived from the slope of regressions of  $A_{\text{water}}$  and  $A_{\text{carbon}}$ .

Variable	$\text{mol H}_2\text{O mol}^{-1} \text{C}^{4+}$	$\text{mol C}^{4+} \text{mol}^{-1} \text{H}_2\text{O}$	$\text{g C}^{4+} \text{Kg}^{-1} \text{H}_2\text{O}$
$WUE_{Pr}$	423.1	0.002	1.3

Table 13. Nutrient contents (% dwb) collected on plant material obtained at harvest in the full beet and lettuce canopy trials. Values are means of three replicates taken of plant material pooled from all chambers, with the exception of beet root, for which only a single sample could be taken due to limited supply of biomass. Bracketed values refer to the standard error of the mean based on n=3. Plant material had to be pooled at harvest to provide sufficient samples for analysis. Beet Tops refers to the leaves and petioles, Beet Bulb refers to the edible, enlarged hypocotyl and Beet Root refers to the fibrous roots for solution uptake. The reported values are % content by mass.

Nutrient	Plant and Part				
	Lettuce (Whole) % dwb	Beet Top % dwb	Beet Bulb % dwb	Beet Root % dwb	Beet Mean % dwb
Nitrogen	5.75 (0.35)	6.14 (0.15)	4.28 (0.02)	5.22	5.21 (0.36)
Calcium	2.19 (0.38)	1.33 (0.11)	0.28 (0.02)	2.61	1.06 (0.33)
Phosphorus	1.10 (0.02)	0.75 (0.01)	0.62 (0.01)	1.12	0.75 (0.07)
Potassium	7.10 (0.28)	10.56 (0.22)	4.75 (0.04)	3.95	7.12 (1.22)
Magnesium	0.69 (0.16)	0.87 (0.07)	0.18 (0.01)	0.97	0.59 (0.15)
Sulphur	0.50 (0.01)	0.38 (0.02)	0.18 (0.00)	0.35	0.29 (0.04)
Ash	28.76 (2.56)	27.24 (0.44)	12.29 (0.09)	26.6	20.74 (2.99)
Organic Carbon	35.62 (1.28)	36.38 (0.22)	43.85 (0.05)	36.7	39.63 (1.50)

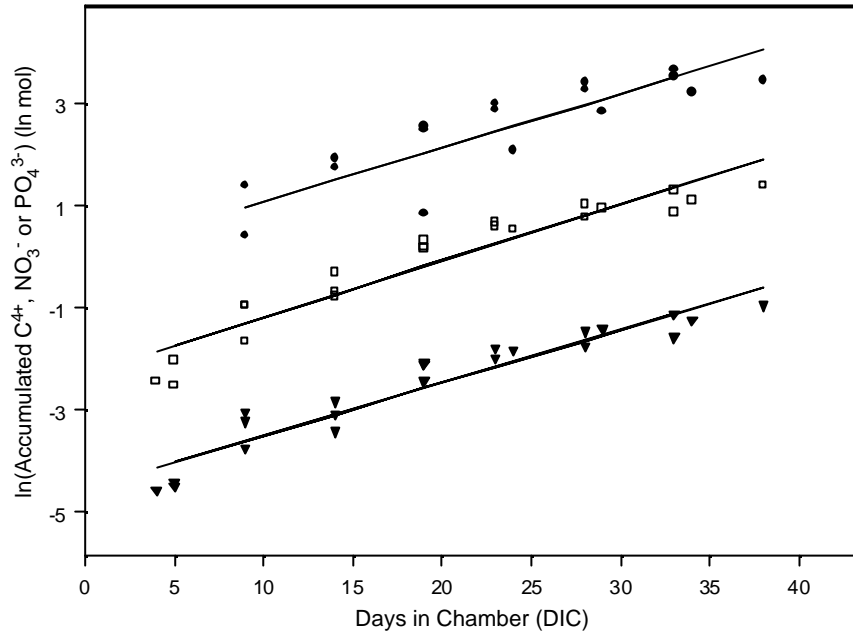


Figure 1. Plot of observed and model fitted ln transform of accumulated carbon (solid circle), nitrate (open square) and phosphate (solid triangle) for all replications of the Beet study. Solid lines indicate the fitted model values.

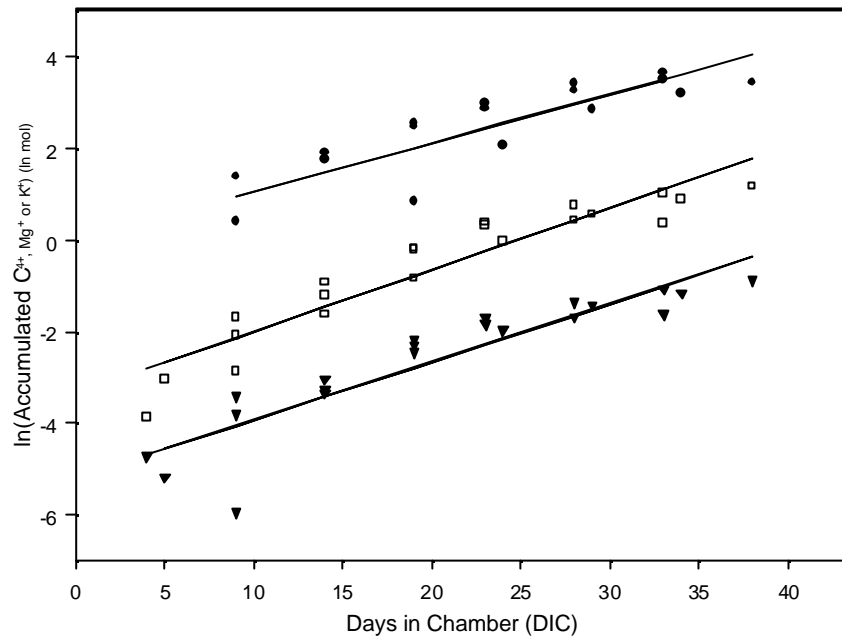


Figure 2. Plot of observed and model fitted ln transform of accumulated carbon (solid circle), potassium (open square) and magnesium (solid triangle) for all replications of the Beet study. Solid lines indicate the fitted model values.

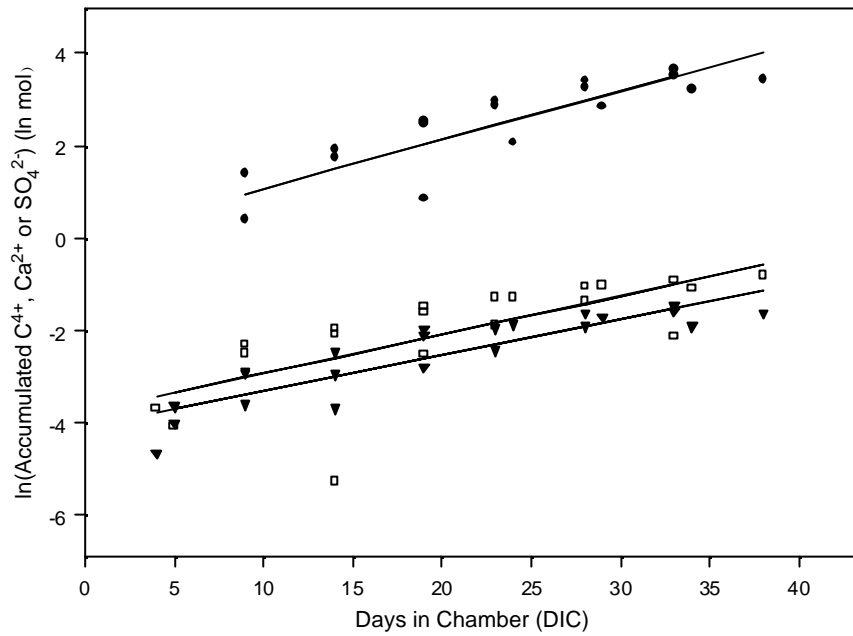


Figure 3. Plot of observed and model fitted ln transform of accumulated carbon (solid circle), calcium (open square) and sulphate (solid triangle) for all replications of the Beet study. Solid lines indicate the fitted model values.



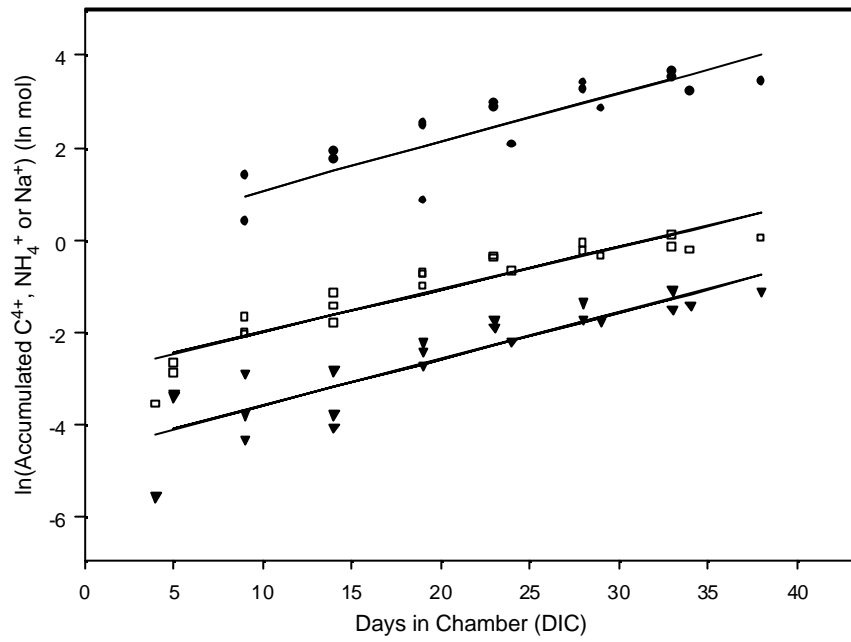


Figure 4. Plot of observed and model fitted  $\ln$  transform of accumulated carbon (solid circle), ammonium (open square) and sodium (solid triangle) for all replications of the Beet study. Solid lines indicate the fitted model values.

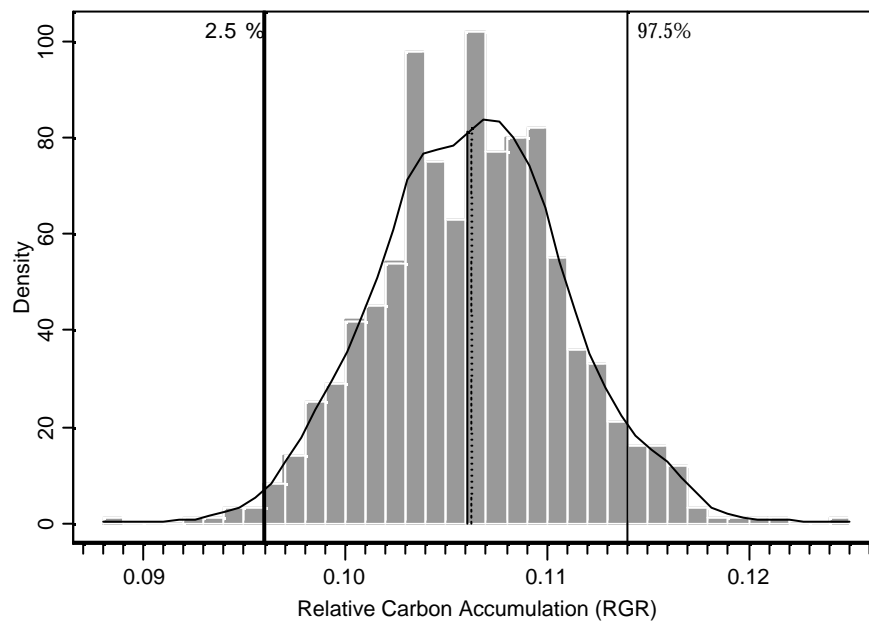


Figure 5. Bootstrap density estimation for relative carbon accumulation (RGR) derived from linear regression on Beet data. Vertical bars indicate the frequency of observed RGR estimates over 1000 iterations of the bootstrap re-sampling procedure. Vertical lines indicate the 2.5% and 97.5% quantiles. The smooth curve is a cubic spline smooth of observed densities.

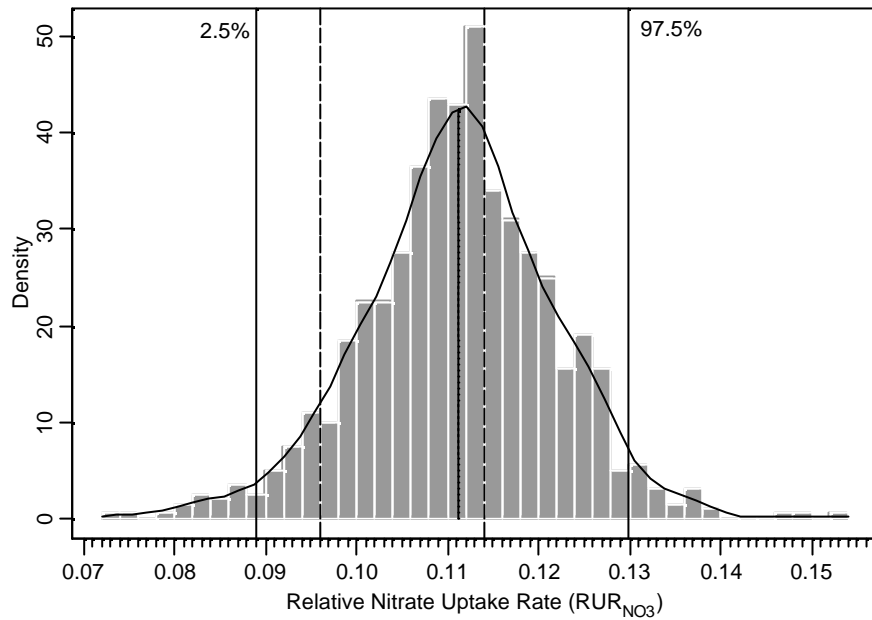


Figure 6. Bootstrap density estimation for relative nitrate uptake ( $RUR_{NO_3}$ ) derived from linear regression on Beet data. Vertical bars indicate the frequency of observed RUR estimates over 1000 iterations of the bootstrap resampling procedure. The solid vertical lines indicate the 2.5% and 97.5% quantiles of the bootstrap estimation on RUR. The smooth curve is a cubic spline smooth of observed densities. The vertical dashed lines are the 2.5% and 97.5% quantiles of the bootstrap estimation on RGR.

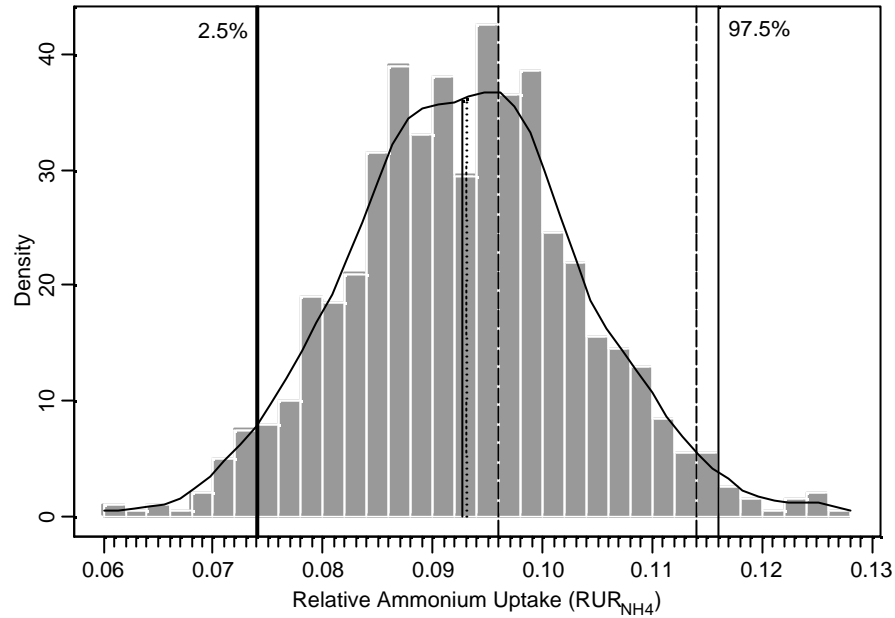


Figure 7. Bootstrap density estimation for relative ammonium uptake ( $RUR_{NH_4}$ ) derived from linear regression on Beet data. Vertical bars indicate the frequency of observed RUR estimates over 1000 iterations of the bootstrap re-sampling procedure. The solid vertical lines indicate the 2.5% and 97.5% quantiles of the bootstrap estimation on RUR. The smooth curve is a cubic spline smooth of observed densities. The vertical dashed lines are the 2.5% and 97.5% quantiles of the bootstrap estimation on RGR.

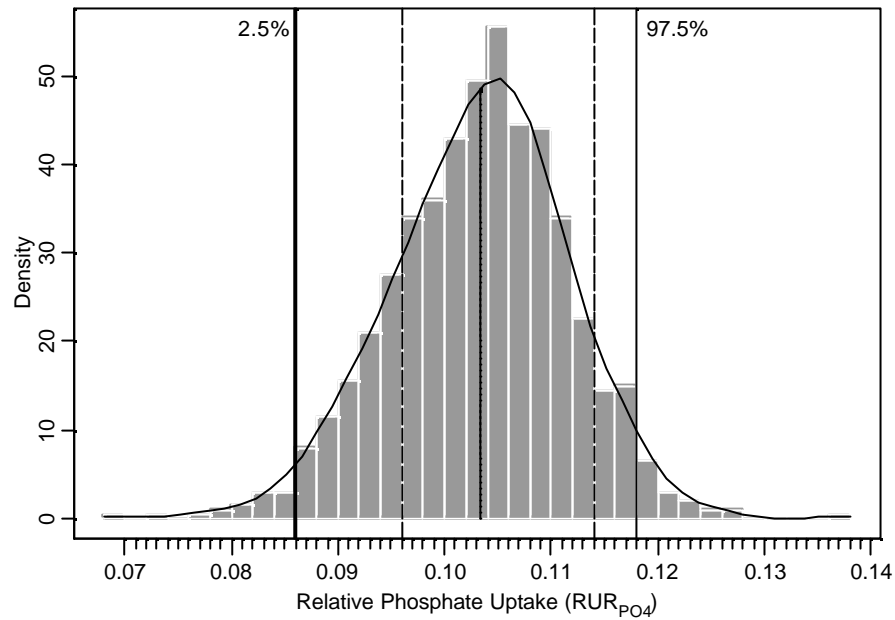


Figure 8. Bootstrap density estimation for relative phosphate uptake ( $RUR_{PO_4}$ ) derived from linear regression on Beet data. Vertical bars indicate the frequency of observed RUR estimates over 1000 iterations of the bootstrap re-sampling procedure. The solid vertical lines indicate the 2.5% and 97.5% quantiles of the bootstrap estimation on RUR. The smooth curve is a cubic spline smooth of observed densities. The vertical dashed lines are the 2.5% and 97.5% quantiles of the bootstrap estimation on RGR.

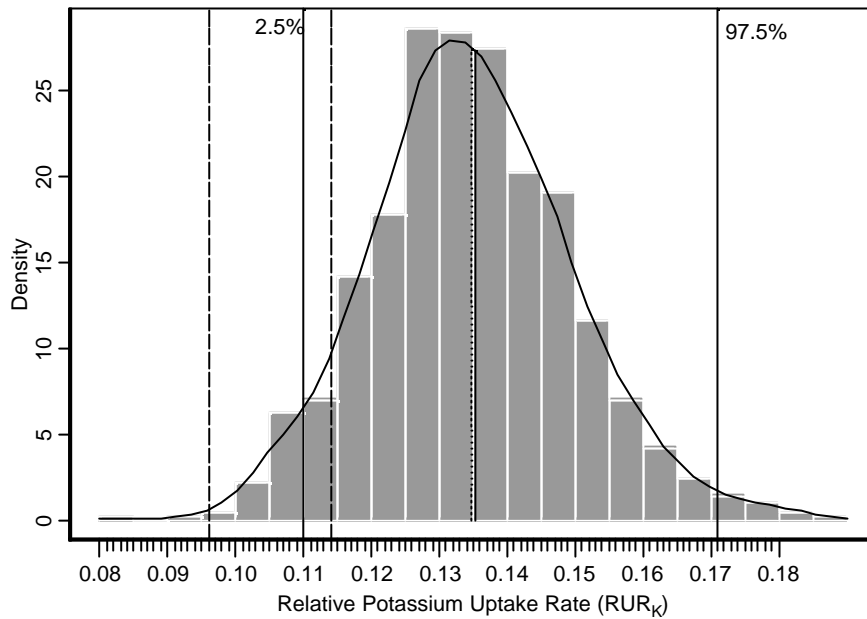


Figure 9. Bootstrap density estimation for relative potassium uptake ( $RUR_K$ ) derived from linear regression on Beet data. Vertical bars indicate the frequency of observed  $RUR$  estimates over 1000 iterations of the bootstrap resampling procedure. The solid vertical lines indicate the 2.5% and 97.5% quantiles of the bootstrap estimation on  $RUR$ . The smooth curve is a cubic spline smooth of observed densities. The vertical dashed lines are the 2.5% and 97.5% quantiles of the bootstrap estimation on  $RGR$ .

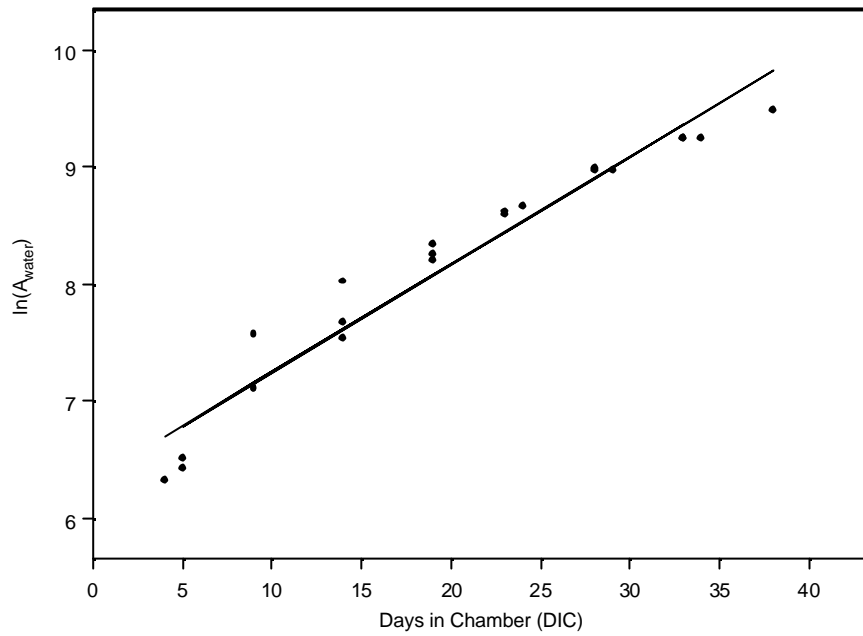


Figure 10. Plot of observed and model fitted  $\ln$  transform of accumulated water use ( $A_{\text{water}}$ , solid circle) for all replications of the Beet study. Solid lines indicate the fitted model values.

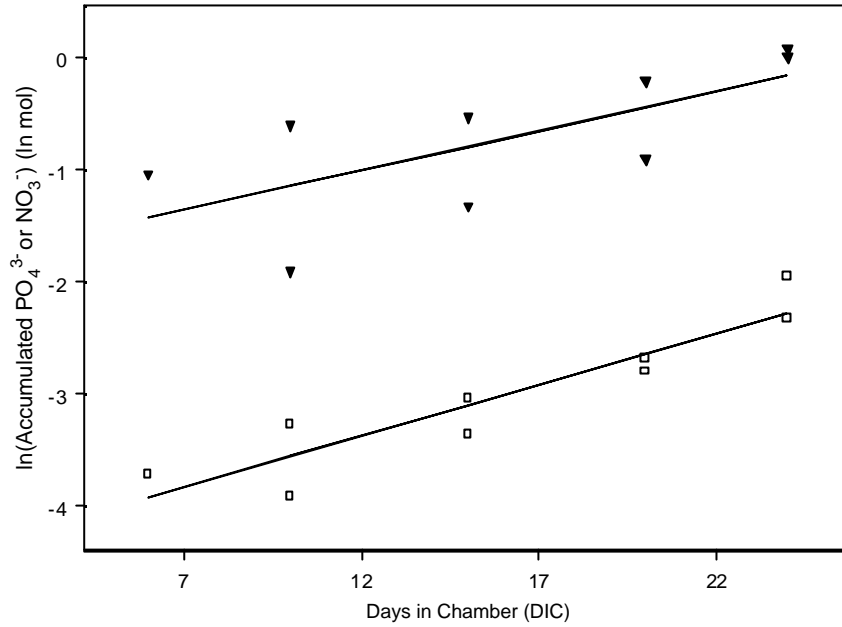


Figure 11. Plot of observed and model fitted ln transform of accumulated phosphate (open square) and nitrate (solid triangle) for all replications of the lettuce study. Solid lines indicate the fitted model values.



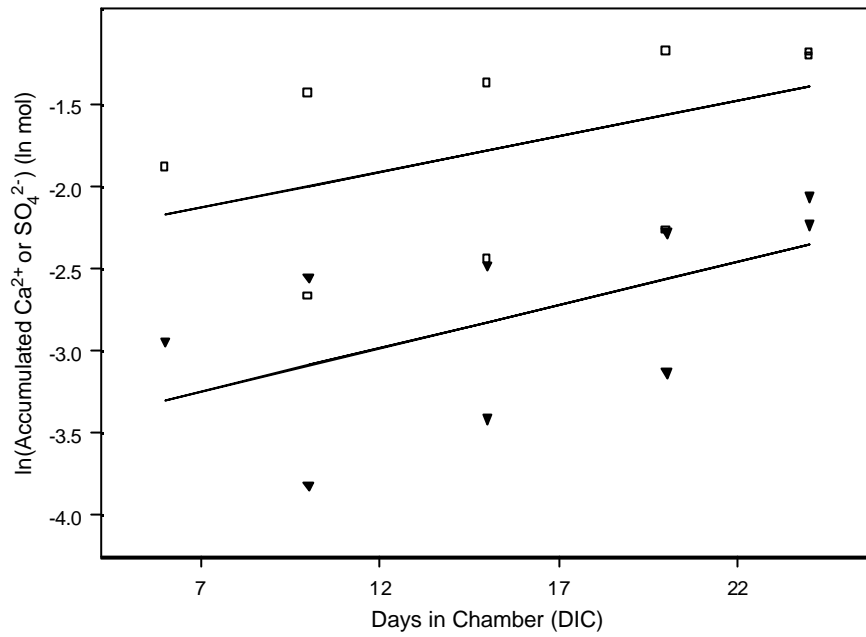


Figure 12. Plot of observed and model fitted ln transform of accumulated calcium (open square) and sulphate (solid triangle) for all replications of the Lettuce study. Solid lines indicate the fitted model values.

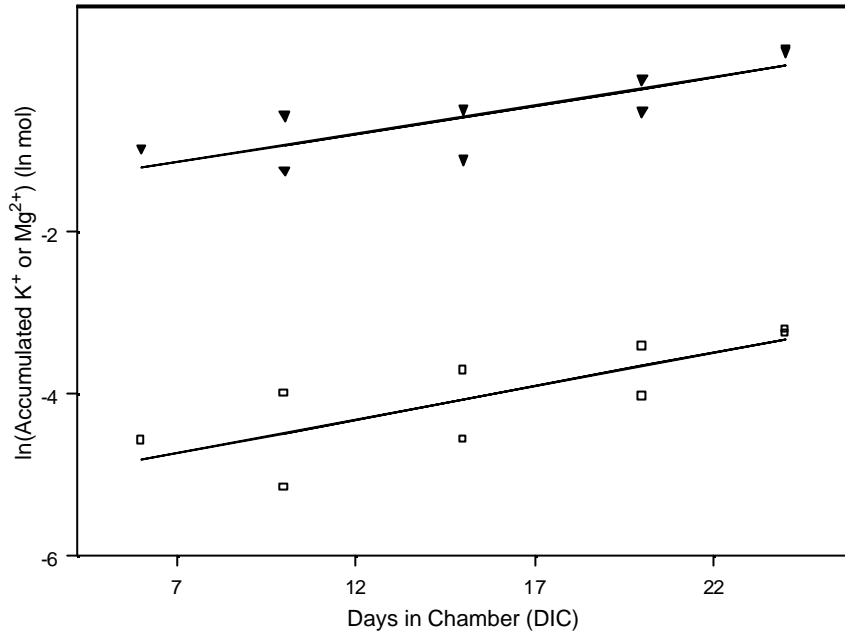


Figure 13. Plot of observed and model fitted ln transform of accumulated magnesium (open square) and potassium (solid triangle) for all replications of the Lettuce study. Solid lines indicate the fitted model values.

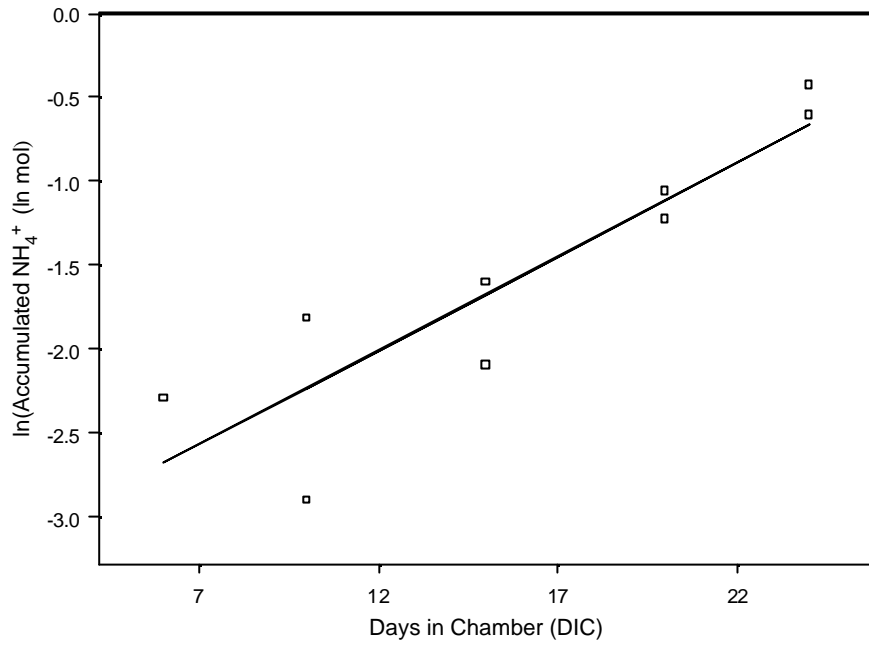


Figure 14. Plot of observed and model fitted ln transform of accumulated ammonium (open square) for all replications of the Lettuce study. Solid lines indicate the fitted model values.

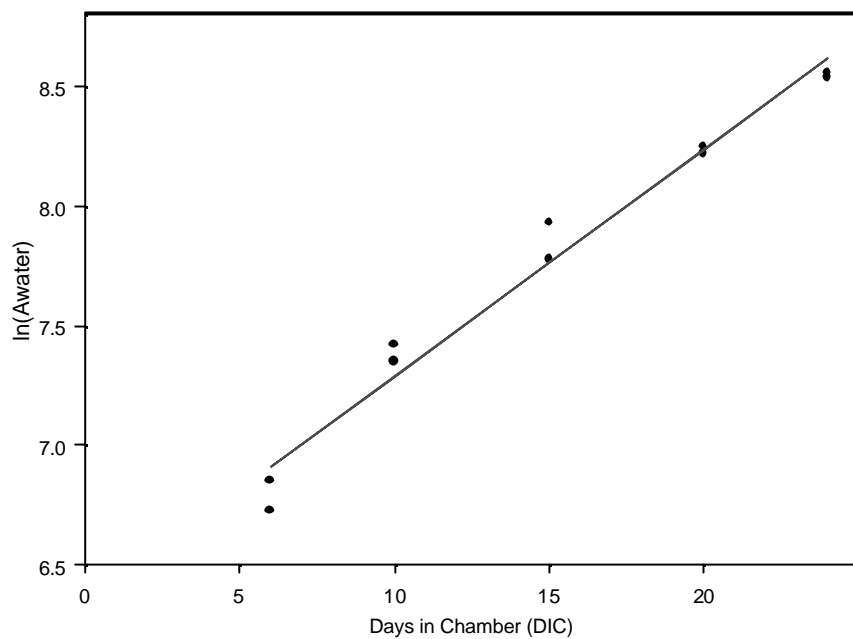


Figure 15. Plot of observed and model fitted  $\ln$  transform of accumulated water use ( $A_{\text{water}}$ , solid circle) for all replications of the Lettuce study. Solid lines indicate the fitted model values.

## Acronyms and Abbreviations

**A<sub>x</sub>** – Accumulated mass of variable x, where x can be water, carbon etc.

**BIO-Plex** – Bioregenerative Planetary Life Support Systems Test Complex

**DAP** – Days After Planting

**DCG** – Daily Carbon Gain

**df** - Degrees of freedom

**DIC** – Days in Chamber

**dwb** – Dry weight basis

**EC** – Electrical Conductivity

**H** – Hat matrix

**h<sub>i</sub>** – Diagonal element of the hat matrix at row i, column i

**Harvest Index (H.I.)** – The ration of edible to total dry biomass of a given crop

**H<sub>o</sub>** – Statistical null hypothesis

**HPC** – Higher Plant Chamber

**LCL** – Lower Confidence Limit (usually 95%)

PF as the independent variable (light curve function)

**n** – Number of observations

**NCER** - Net Carbon Exchange Rate

**f** - Cumulative distribution function of the standard normal distribution

**p** – Number of estimated parameters in a regression model

**PPF** – Photosynthetic Photon Flux

**RGR(t)** - Relative Growth Rate function of time, t

**RUR(t)** - Relative Uptake Rate as a function of time, t

**RUR<sub>η</sub>** - Relative Uptake Rate of any ion, η.

$r_i^*$  - Studentized residual

$r_i'$  – Standardized residual

$r(i)$  – Deletion residual

**SLSR** – Simple Least Squares Regression

$t$  – Time

**UCL** – Upper Confidence Limit (usually 95%)

$U_{\eta}(t)$  - Instantaneous uptake rate, at time  $t$ , for nutrient  $\eta$ ?

$W(t)$  – Accumulated biomass at time,  $t$

$WUE_{Pr}$  – Water Use Efficiency of Productivity

$X$  – Matrix of independent variables

## Appendix 1

### Full Canopy Chamber Schematic and Experimental Design for Batch Stand Trials

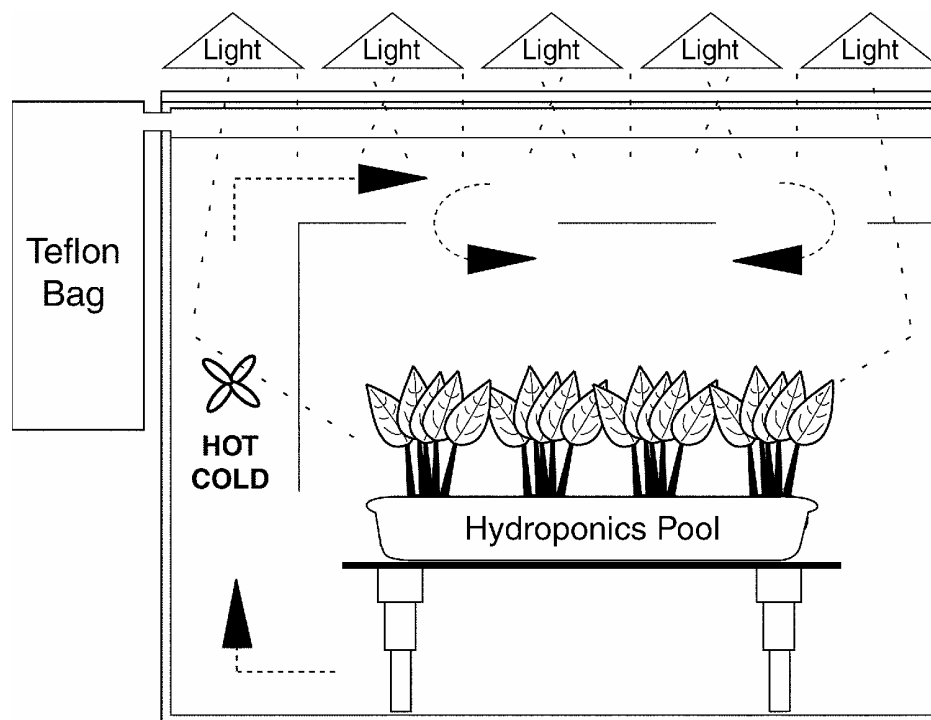


Figure A1.1. Schematic representation of full canopy chambers used in batch stand studies. Shown are the even aged crops, hydroponics pool, lighting system and Teflon bags to maintain ambient pressure.